Received: 2 August 2022 | Revised: 27 September 2022 | Accepted: 31 October 2022

IET Generation, Transmission & Distribution

DOI: 10.1049/gtd2.12702

ORIGINAL RESEARCH

A novel energy management model among interdependent sections in the smart grids

Ali Maroufi[1] | Mohammadamin Mobtahej[2] | Mazaher Karimi[3] | Aliasghar Baziar[4]

[1]ITCEN Consulting Engineers, Tehran, Iran

[2]School of Electrical Engineering, Kazeroon Islamic Azad University, Fars, Iran

[3]School of Technology and Innovations, University of Vaasa, Wolffintie 34, Vaasa, Finland

[4]PEDC Company, Pasargad Energy Development Company, Shiraz, Iran

Correspondence
Mohammadamin Mobtahej, School of Electrical Engineering, Kazeroon Islamic Azad University, Fars 652041, Iran.
Email: Aminmobtahej@gmail.com

Abstract

Technically, residential energy management systems are fundamental sectors in the smart grids for implementing demand response programs in the layer of households for managing energy consumption and reducing energy bills. The paper proposes a novel energy management scheme that takes production and usage into account based on a heuristic searching operation. In addition to modelling the grid, renewable energy sources, batteries, and electric vehicles, various kinds of electrical and thermal devices have been examined, including air conditioners, water heaters, vacuum cleaners etc. A method is developed for solving the objective constraint issue in a smart home in order to reduce energy consumption and determine feasible operation states among the various loads. Moreover, this paper proposes a grey wolf optimization method for solving the issue over a longer simulation period. Various cases were examined to evaluate the effectiveness of this suggested robust optimization algorithm. The outcomes show that the suggested model could not only reduce energy costs significantly but has also shown good performance for energy management purposes.

1 | INTRODUCTION

Smart grids (SGs) improve reliability, increase renewable energy consumption and respond quickly to user needs. As renewable generators (such as wind and solar) and distributed traditional generators have become part of the grid, SGs are being faced with numerous problems [1, 2]. SGs face a problem in terms of economics. As electricity networks contain several traditional and renewable generators, along with non-dispatchable and dispatchable loads, the economic operation of SGs requires optimized management both on the supply side and the demand side. It is traditional for economic dispatch and demand response (DR) to be operated independently. The economic dispatch seeks to allocate energy production economically between generators and maintains continuous respect for the system's physical limitations. Traditional economic dispatch makes the assumption that load requirements will remain stationary. Power systems and markets are increasingly reliant on DR [3]. In addition to helping consumers make good decisions about their power usage, it also will decrease the total peak load demand, change the demand profile and enhance the sustainability of the network. The current DR applications have been constructed for following defined load curves or pricing schemes [4] or eliminating a predetermined amount of loads based on a schedule [5].

In one sense, traditional generators must modify their output when operational conditions change, for example, when renewable energy production varies. Allocations between them need to be redistributed economically. Conversely, users adjust their needs according to their profit functions for maximizing their profits in response to market prices [6]. As both economic dispatch and DR participate in energy markets, their operations would be affected by one another. By operating DR, the load profiles would be reshaped, so the productions would be different from the initial optimum point reached by the economic dispatch, requiring a second round of economic dispatch. As a result of economic dispatch, the market pricing changes, activating DR. The economic dispatch and DR have been closely linked and must be considered when managing power online. The interactive method takes a considerable time for convergence when economic dispatch and DR operate separately. Therefore, it would be essential to take into account the

interactions between economic dispatch and DR and to address them as an integrated system.

Two types of conventional algorithms are used to solve economic dispatch or DR problems. Analytical techniques, including Lagrange multipliers [7], gradient search methods [8], and linear programming [9], fall into group one. In the next group are heuristic methods including genetic algorithms [10], evolutionary programming [11], particle swarm optimization [12] and so on. The majority of these approaches have been centralized and implemented on a large scale. Centralized solutions tend to be less flexible and prone to single-point failures [13]. They require complex communication systems for collecting global data, as well as highly efficient central controllers for processing enormous information. Therefore, such approaches might have difficulty responding fast enough, for instance, when operational modes change rapidly, like ones caused by unpredictability and uncertainties in renewable energy sources. These solutions must therefore improve their response speeds.

Many distributed approaches are suggested as a means of addressing the shortcomings of centralized solutions. Ref. [14] offered a DR technique involving optimization of utilities. Despite the fact that the study's bidding procedure is distributed, there is also the need for a central controller for collecting demand data from users for determining market prices. Ref. [15] examined an increasing price consensus algorithm to solve the economic dispatch issue on a distributed basis. Although economic dispatch is considered in that approach, DR is not. Ref. [16] examined a population dynamics method for dispatching distributed generators in SGs. Even so, auctioneer agents working as centralized coordinators are vitally needed. The intermittent renewable production did not appear to be taken into account in any of those studies. As renewable energy generators are increasingly incorporated into the energy grid and as consumers become more involved in energy markets, it is imperative to develop effective distributed algorithms for integrated optimum energy management (EM) taking generators and consumers into account. There were several studies that failed to take into account various renewable energy sources with some neglecting power generation management. Most of them failed to incorporate electric vehicles (EVs) with vehicle-to-grid (V2G) capabilities, which is important for smart homes (SHs). Many studies fail to implement an optimization algorithm for several successive days, and not just for one day-ahead simulation. Only a few investigations are conducted on EMS for SHs, which can schedule and control various kinds of electrical and thermal devices.

The study presents an EM scheme and mathematical modelling methods for the network, renewable energy sources, batteries, EVs, and various kinds of electrical and thermal devices. This paper implements an accurate solution strategy for reducing the energy costs in SHs and determining the operational states for various loads, next proposes a mixed-integer linear programming model according to a grey wolf optimization algorithm (GWOA) for solving the issue over a long simulation time period. In the study, the following main contributions are presented: (1) This paper implements a precise solution approach for minimizing the energy price in SHs through the schedule and control of generation systems and both electrical and thermal loads while considering specific preferred appliance temperatures chosen by users. (2) This study proposes the GWOA, considering multiple restrictions, in order to address the issue over a longer simulation period. (3) This suggested optimization algorithm was evaluated via numerous simulations with various cases to show that the energy price was significantly reduced and that this suggested optimization method was effective.

Following is a summary of the remaining sections. Section 2 describes the SH system in which various generation and usage systems are integrated. Section 3 develops the problem definition with each of the limitations associated with every system. The GWOA would solve the issue over a longer simulation period is presented in Section 4, which describes the optimization methods that are employed for optimizing the electrical SG and its components. Section 5 discusses simulation outcomes. Section 6 analyses the effectiveness of this suggested optimization algorithm, and Section 7 presents a conclusion.

2 | PROPOSED SH MODELLING

This section explains the model and formulations required for handling the proposed problem. In the paper, the suggested optimization algorithm has been designed for reducing power consumption costs for day-ahead and long-term simulations through the control of certain loads based on predetermined devices' temperatures and by switching to times with lower tariffs. Smart devices would be categorized into two main groups in the proposed SH system:

1. Electrical controllable loads (ECL) like cooker hoods, vacuum cleaners, washing machines and so on.
2. Thermal controllable (TCL) loads like refrigerators (REF), air conditioning (AC) and electric water heaters (EWH).

Table 1 [17] shows various ECL and TCL parameters, including the first start time and the last finish time, as well as energy usage and period. Moreover, energy production management must be taken into account. As a result of the perfect alignment of such resources, a home photovoltaic (PV) system and a micro wind turbine (WT) were integrated beside the traditional power plant. In addition, electric batteries and 2 EVs will be added to the SH since ref. [18] shows that the optimal solution would be to use two EVs within a similarly planned structure. The weather forecast provides 24-h information on solar radiation and wind speed. In this model, horizon T and time step t are considered. 1 h can be used as a time slot, so every day will consist of 24 slots. Figure 1 shows the model of the SH.

3 | PROBLEM FORMULA

In order to solve the problem properly, it is needed to suggest an MILP model for EM over the period T with t time steps. Time

TABLE 1 Electrical house devices characteristics

Devices	Dryer	Oven	Cooker hood	TV	Desktop	Laptop	Iron	Microwave	Radio player
Kind	ECL	ECL	ECL	ECL	ECL	ECL	ECL	ECL	ECL
Earliest start time (h)	13	15	17	19	14	14	5	7	7
Final finish time (h)	18	19	19	24	24	24	20	9	8
Time window (h)	5	4	2	5	10	10	15	2	1
Duration (h)	1	2	1	5	5	3	2	1	1
Power (kW)	2.5	2.5	0.2	0.3	0.3	0.1	2.7	1.7	0.2
Devices	**Sensors**	**Dish washer**	**Water heater**	**AC**	**Illumination**	**Vacuum cleaner**	**REF**	**Washing machine**	**Other occasional loads**
Kind	ECL	ECL	TCL	TCL	ECL	ECL	TCL	ECL	ECL
Earliest start time (h)	0	9	24	12	19	7	0	9	0
Final finish time (h)	24	17	0	24	25	20	24	12	24
Time window (h)	24	8	24	12	5	13	24	3	24
Duration (h)	24	1	1	12	5	1	24	2	5
Power (kW)	0.01	1.7	1.7	1.15	0.5	2	0.175	1.8	3

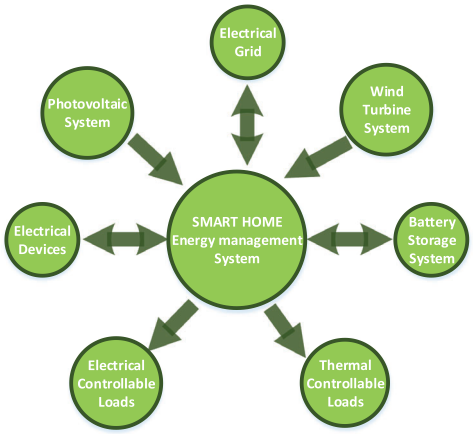

FIGURE 1 SH framework

slots are assumed to be 1 h, so there are 24 slots per day. Here would be the formulas describing the related limitations.

3.1 | Electrical controllable loads

The electrical devices should be operated within the specified timeframe:

$$\begin{cases} V\ (t,i) = 0\ if\ t\ \langle T_{start}\ (i)\ \ and\ t\rangle\ T_{finish\ h}\ (i) \\ V\ (t,i) = T_{treat}\ \ (i)\ \ if\ t \geq T_{start}\ (i)\ \ and\ t \leq T_{finish\ h}\ (i) \end{cases} \tag{1}$$

In which, i shows the index of house devices and t indicates time period. $V(t,i)$ indicates the status of beginning of device i in t (1 = device i begins). $T_{treat}(i)$ shows the run time of device i, $T_{start}(i)$ indicates the first start time of device i, and $T_{finish\ h}(i)$ shows the last finish time of device i.

3.2 | Thermal controllable loads

3.2.1 | Air conditioning

When the AC is in the cooling state, it operates as follows:

$$T_{ins}\ (t) = (\in \times T_{ins}\ (t-1)) + (1-\ ) \times \left(T_{out}\ (t) - \left(\frac{\mu \times B^{c}_{ac}\ (t) \times P_{ac}}{\mathcal{A}} \right) \right) \tag{2}$$

$T_{ins}(t)$ is the inside room temperature in t. $T_{out}(t)$ shows the outside temperature in t. The coefficient of efficiency of the AC is shown by μ and the system inertia is shown by $\in$. P_{ac} shows the energy usage of the AC. $B^{c}_{ac}(t)$ indicates the status of the AC in t (1 = AC turn on in cooling status). The thermal conductivity of the construction has been shown by $\mathcal{A}$. When the AC is in the heating state, it operates as follows:

$$T_{ins}\ (t) = (\in \times T_{ins}\ (t-1)) + (1-\in) \times \left(T_{out}\ (t) - \left(\frac{\mu \times B^{h}_{ac}\ (t) \times P_{ac}}{\mathcal{A}} \right) \right) \tag{3}$$

$B^{h}_{ac}(t)$ shows the mode of the AC in t (1 = AC turn on in heating state). Activation and deactivation cannot be done at the

same time:

$$B_{ac}^{c}(t) + B_{ac}^{h}(t) \leq 1 \tag{4}$$

Within the acceptable range, the inside temperature is limited as follows:

$$T_{ins}^{\min\_des}(t) \leq T_{ins}(t) \leq T_{ins}^{\max\_des}(t) \tag{5}$$

$T_{ins}^{\max\_des}(t)$ shows the lower acceptable bound of inside room temperature in t and $T_{ins}^{\min\_des}(t)$ indicates the upper acceptable bound of inside room temperature in t. Status to activate the AC in cooling status:

$$B_{ac}^{c}(t) = \begin{cases} 0 \; if \; T_{ins}(0) < T_{ins}^{\min\_des}(1) \\ 1 \; if \; T_{ins}(0) > T_{ins}^{\max\_des}(1) \end{cases} \tag{6}$$

Status to activate the AC in heating Status:

$$B_{ac}^{h}(t) = \begin{cases} 1 \; if \; T_{ins}(0) < T_{ins}^{\min\_des}(1) \\ 0 \; if \; T_{ins}(0) > T_{ins}^{\max\_des}(1) \end{cases} \tag{7}$$

AC operates in the cooling state during the following time period:

$$B_{ac}^{c}(t) = \begin{cases} 0 \; or \; 1 \; if \; t \in T_C \\ 0 \qquad if \; t \notin T_C \end{cases} \tag{8}$$

AC operates in the heating state during the following time period:

$$B_{ac}^{h}(t) = \begin{cases} 0 \; or \; 1 \; if \; t \in T_H \\ 0 \qquad if \; t \notin T_H \end{cases} \tag{9}$$

3.2.2 | Refrigerators (REF)

The REF operates as follows:

$$T_{ref}(t) = T_{ref}(t) + dt\left(\left(B_{ref} \times P_{ref}\right) - \left(\alpha_{ref}(t) \times B_{ref}(t)\right) + \gamma_{ref}\right) \tag{10}$$

B_{ref} shows the effect of activity likelihood on the REF temperature and $\alpha_{ref}(t)$ indicates the effect of the ON and OFF modes on the REF temperature. The energy usage of the REF is shown byP_{ref}. $T_{ref}(t)$ shows the REF temperature in t. $B_{ref}(t)$ shows the mode of the REF in t (1 = REF turn on). The thermal leakage of REF has been shown by γ_{ref}. The temperature of the REF must be limited to the preferred range:

$$T_{ref}^{\min\_des}(t) \leq T_{ref}(t) \leq T_{ref}^{\max\_des}(t) \tag{11}$$

$T_{ref}^{\max\_des}(t)$ shows the upper preferred bound of Ref temperature in t and $T_{ref}^{\min\_des}(t)$ indicates the lower preferred bound of REF temperature in t. Mode to activate the REF:

$$B_{ref}(t) = \begin{cases} 1 \quad if \; T_{ref}(0) > T_{ref}^{\max\_des}(1) \\ 0 \quad if \; T_{ref}(0) < T_{ref}^{\min\_des}(1) \end{cases} \tag{12}$$

3.2.3 | Electric water heater (EWH)

The EWH operates as follows:

$$C_{ewh} \times \left(\frac{T_{ewh}(t) - T_{ewh}(t-1)}{dt}\right) = \frac{-1}{R_{ewh}} \times \left(T_{ewh}(t) - T_{ins}(t)\right) + \left(B_{ewh}(t) \times P_{ewh}\right) - \left(c_p \times q \times \left(T_{ewh}^{max-des}(t) - T_{ewh}^{cold}\right)\right) \tag{13}$$

The tank thermal capacity of EWH is shown by C_{ewh}. The water temperature of EWH in t has been shown by $T_{ewh}(t)$. T_{ewh}^{cold} shows the temperature of the incoming water into the EWH. $T_{ewh}^{max-des}(t)$ indicates the upper preferred temperature bound of EWH in t and $T_{ewh}^{min-des}(t)$ shows the lower preferred temperature bound of EWH in t. The certain heat constant for water of EWH has been shown byc_p. q shows the hot water flow of EWH. $B_{ewh}(t)$ indicates the mode of the EWH in t (1 = EWH turn on). The thermal resistance of tank walls of EWH has been shown by R_{ewh}. The energy usage of the EWH has been shown by P_{ewh}.

The temperature of the water must be limited to the preferred range:

$$T_{ewh}^{\min\_des}(t) \leq T_{ewh}(t) \leq T_{ewh}^{\max\_des}(t) \tag{14}$$

Mode to activate the EWH:

$$B_{ewh}(t) = \begin{cases} 0 \; if \; T_{ewh}(0) > T_{ewh}^{\max\_des}(1) \\ 1 \; if \; T_{ewh}(0) < T_{ewh}^{\min\_des}(1) \end{cases} \tag{15}$$

3.3 | Electric grid

The bounds of energy imported from the system are as follows:

$$0 \leq P_{Grid}(t) \leq P_{Grid}^{max} \tag{16}$$

$P_{Grid}(t)$ defines the energy imported from the system in t and P_{Grid}^{max}shows the utmost imported energy from the system in t.

3.4 | PV system

The bounds of energy produced via PV are as follows:

$$0 \leq P_{PV}(t) \leq P_{PV}^{max} \tag{17}$$

$P_{PV}(t)$ is the energy produced via the PV system in t and P_{PV}^{max} shows the utmost permitted PV energy in t. The produced output energy from PV is as follows [19]:

$$P_{PV}(t) \leq A_{PV} \times \rho \times SI(t) \tag{18}$$

A_{PV} shows the area of PV. The performance of PV has been shown by ρ. $SI(t)$ shows the solar irradiation in t.

3.5 | Wind turbine (WT)

The bounds of the energy produced via wind system are as follows:

$$0 \leq P_W(t) \leq P_W^{max} \tag{19}$$

$P_W(t)$ shows the energy produced via the wind system in t and P_W^{max} indicates the utmost permitted wind power in t. The produced output energy from wind system is as follows [20]:

$$\begin{cases} P_W(t) = 0 \text{ if} v_f \left\langle v_{ci} \text{ and } v_f \right\rangle v_{co} \\ P_W(t) = P_{rated} \text{ if} v_r \leq v_f \leq v_{co} \\ P_W(t) = P_{rated} \times \dfrac{v_f - v_{ci}}{v_r - v_{ci}} \; if v_{ci} \leq v_f \leq v_r \end{cases} \tag{20}$$

P_{rated} shows the rated energy of the wind system. v_f shows the prediction wind speed, v_r shows the rated speed of the WT, v_{ci} indicates the cut-in speed of the WT and v_{co} shows the cut-off speed of the WT.

3.6 | Battery storage system (BSS)

The bounds of permitted charging energy are as follows:

$$P_B^{Ch}(t) \leq P_B^{Cmax} \times Y(t) \tag{21}$$

$P_B^{Ch}(t)$ indicates the energy charging BSS in t, and P_B^{Cmax} shows the utmost permitted energy charging of battery. $Y(t)$ shows the mode of the battery in t (1 = charging).

The limit of allowed discharging power:

$$P_B^{Disch}(t) \leq P_B^{Dmax} \times Z(t) \tag{22}$$

$P_B^{Disch}(t)$ indicates the discharging energy from battery in t and P_B^{Dmax} shows the utmost permitted energy discharging of battery. $Z(t)$ shows the mode of the battery in t (1 = discharging).

Charging and discharging cannot be done at the same time:

$$Y(t) + Z(t) \leq 1 \tag{23}$$

Energy saved in the battery for $t > 1$:

$$Nom_B \times SOC_B(t) = Nom_B \times SOC_B(t-1) + \left(\frac{P_B^{Ch}(t) \times dt}{e_c} - \left(e_d \times P_B^{Disch}(t) \times dt \right) \right) \tag{24}$$

Nom_B shows the battery nominal capacity. $SOC_B(t)$ indicates the mode of charging of the battery in t. e_c indicates the charge coefficient factor and e_d shows the discharge coefficient factor.

This is the battery's earliest status:

$$Nom_B \times SOC_B(1) = Nom_B^{int} \left(\frac{P_B^{Ch}(1) \times dt}{e_c} - \left(e_d \times P_B^{Disch}(1) \times dt \right) \right) \tag{25}$$

Here, Nom_B^{int} shows the first battery capacity.

Limit of mode of charging of the battery is as follows:

$$SOC_B^{min} \leq SOC_B(t) \leq 1 \tag{26}$$

Utmost battery charging bound is as follows:

$$\frac{P_B^{Ch}(1) \times dt}{e_c} - (Nom_B \times SOC_B(t-1)) \leq Nom_B \tag{27}$$

3.7 | Electric vehicles

The bounds of permitted charge energy are as follows:

$$\begin{cases} P_{EV}^{Ch}(t,j) \leq P_{EV}^{Cmax}(j) \times W(t,j) \;\; \forall t \in T_{stay} \\ P_{EV}^{Ch}(t,j) = 0 \;\; \forall t \notin T_{stay} \end{cases} \tag{28}$$

where j indicates the index of EVs. $P_{EV}^{Cmax}(j)$ is the utmost permitted energy charging of EV battery j and $P_{EV}^{Ch}(t,j)$ shows the energy charging by EV j in t. $W(t,j)$ shows the mode of the EV battery j in t (1 = charging). Limit of permitted discharge energy and EV travel demand:

$$\begin{cases} P_{EV}^{Disch}(t,j) \leq P_{EV}^{Dmax}(j) \times X(t,j) \;\; \forall t \in [1,\ldots,T] \\ P_{EV}^{Disch}(t,j) \times dt = D_{EVdriv}(t,j) \;\; \forall t \notin T_{stay} \end{cases} \tag{29}$$

$P_{EV}^{Disch}(t,j)$ indicates the discharging energy from EV j in t and $P_{EV}^{Dmax}(j)$ shows the utmost permitted energy discharging of EV battery j. $X(t,j)$ shows the mode of the EV battery j in t (1 = discharging). T defines the set of optimization time period and T_{stay} shows the set of interval whenever electrical devices are at house. $D_{EVdrive}(t,j)$ shows the driving electricity demand of EV j in t.

Charging and discharging cannot be done at the same time:

$$W(t,j) + X(t,j) \leq 1 \tag{30}$$

Energy saved in the EV battery for $t > 1$:

$$Nom_{EV}(j) \times SOC_{EV}(t,j) = Nom_{EV}(j) \times SOC_{EV}(t-1,j) + \left(\frac{P_B^{Ch}(t,j) \times dt}{e_c} - \left(e_d \times P_{EV}^{Disch}(t,j) \times dt \right) \right) \tag{31}$$

in which, $Nom_{EV}(j)$ shows the nominal capacity of electrical device battery j.

The earliest mode of EV battery is as follows:

$$Nom_{EV}(j) \times SOC_{EV}(t,1) = Nom_{EV}^{int}(j) + \left(\frac{P_{EV}^{Ch}(1,j) \times dt}{e_c} - \left(e_d \times P_{EV}^{Disch}(1,j) \times dt \right) \right) \tag{32}$$

in which, $Nom_{EV}^{int}(j)$ shows the first capacity of electrical device battery j.

Bound of mode of charging of EV battery is as follows:

$$SOC_{EV}^{min}(j) \leq SOC_{EV}(t,j) \leq 1 \tag{33}$$

in which, $SOC_{EV}^{min}(j)$ shows the minimal mode of charging of EV battery and $SOC_{EV}(t,j)$ indicates the mode of charging of the EV battery j in t.

The utmost EV battery charging bound is as follows:

$$\frac{P_{EV}^{Ch}(t,j) \times dt}{e_c} - (Nom_{EV}(j) \times SOC_{EV}(t-1,1)) \leq Nom_{EV}(j) \tag{34}$$

3.8 | Grid power balance

Balance among usage and generation must be guaranteed by the distribution system:

$$P_{Grid}(t) + P_{PV}(t) + P_W(t) + \sum_j^{N_{EV}} P_{EV}^{Disch}(t,j) + P_B^{Disch}(t) = \sum_i \left(D_{appl}(i) \times V(i,t) \right) + D_{th}(t) + \sum_j^{N_{EV}} P_{EV}^{Ch}(t,j) + P_{inject}(t) \tag{35}$$

$D_{appl}(i)$ defines the constant energy usage of device i, $D_{th}(t)$ shows the energy usage of thermal controllable loads in t and $P_{inject}(t)$ indicates the amount of energy selling to the grid in t. N_{EV} shows the whole number of electrical devices.

Injecting into the system at the same time as EV batteries are being discharged is prohibited:

$$P_{inject}(t) \leq P_{inject}^{max} \times M(t) \tag{36}$$

$$P_{Grid}(t) \leq P_{Grid}^{max} \times N(t) \tag{37}$$

$$M(t) + N(t) \leq 1 \tag{38}$$

$$M(t) + X(t,j) \leq 1 \tag{39}$$

$$M(t) + Z(t) \leq 1 \tag{40}$$

$M(t)$ indicates the mode of the injecting into the system in t and $N(t)$ shows the mode of the grid generation in t. N_{EV} shows the overall number of EVs. The equality has been guaranteed in case of $t \in T_{stay}$ (T_{stay} = interval whenever EV remains at house), if not, the EV power must be eliminated from the formula since this study assumes there was no charge procedure for the electrical device if it was not at home.

3.9 | Objective function

The objective function of the system can be determined in the following way:

$$\begin{aligned} min\, f(cost) = \sum \Bigg\{ & \left[(P_{Grid}(t) \times dt) \times C_{Grid}(t) \right] \\ & + \left[(P_{PV}(t) \times dt) \times C_{PV} \right] + \left[(P_W(t) \times dt) C_W \right] \\ & + \left[\sum_j^{N_{EV}} (P_{EV}^{Disch}(t,j) \times dt) \times C_{EV}^{Disch} \right] \\ & + \left[\left(P_B^{Disch}(t) \times dt \right) \times C_B^{Disch} \right] \\ & - \left[\left(P_{inject}(t) \times dt \right) \times C_{Sell} \right] \Bigg\} \end{aligned} \tag{41}$$

where f shows the objective function of the optimization problem. $C_{Grid}(t)$ shows the price of energy produced via the grid in t, $C_{PV}(t)$ shows the production and maintenance price of PV in t, $C_W(t)$ shows the production and maintenance price of wind system in t, $C_{EV}^{Disch}(t)$ indicates the maintenance price of electrical device in t, and $C_B^{Disch}(t)$ shows the maintenance price of BSS in t.

Its goal is to reduce residential consumers' day-ahead energy bills.

4 | THE IMPROVED GWOA

As explained before, the proposed problem has a non-linear and complex structure which needs to get solved in a proper way. This paper proposes the MGWOA here for making exploration and exploitation more effective by improving the randomized nature of the existing algorithm. In the GWOA iteration procedure, α indicates the solution with the highest fitness, β shows the second optimum solution and δ represents third optimum solution, and ω refers to all other possible solutions. There are two basic parts of the GWOA: encircling and hunting the target. Encircling is expressed as follows [21]:

$$\vec{D} = \left|\vec{C} \cdot \vec{X}_p(k) - \vec{X}(k)\right| \tag{42}$$

$$\vec{X}(k+1) = \vec{X}_p(k) - \vec{A}.\vec{D} \tag{43}$$

In which, the existing iteration has been shown by k, the place vector of target has been shown by $\vec{X}_p$, the place vector of the grey wolves has been shown by $\vec{X}$ · $\vec{C}$ and $\vec{A}$ show the randomly selected coefficients vectors and are determined as follows:

$$\vec{A} = 2\vec{a} \cdot \vec{r}_1 - \vec{a} \tag{44}$$

$$\vec{C} = 2 \cdot \vec{r}_2 \tag{45}$$

$\vec{r}_1$ and $\vec{r}_2$ show randomly selected variables among 0 and 1 in each iteration. $\vec{a}$ reduces from 2 to 0 linearly with increasing iterations in the base GWO, resulting in a direct effect on $\vec{A}$. The search space is explored if $|\vec{A}| > 1$ and the exploitation trend is enhanced if $|\vec{A}| < 1$ [22]. In MGWO, a non-linear $\vec{a}$ has been used for improving agents' exploring capabilities during the first iterations:

$$\vec{a} = 2 \cdot \cos(k/Max_k) \tag{46}$$

In which, the utmost iteration number is shown by Max_k. Main GWOA updates and stores α, β and δ during all iterations. Based on the three optimum position vectors, the rest of the search agents (like Omega wolves) must update their location vectors. The updating procedure is described by these formulas:

$$\vec{D}_\alpha = \left|\vec{C}_1 \cdot \vec{X}_\alpha - \vec{X}\right| \tag{47}$$

$$\vec{D}_\beta = \left|\vec{C}_2 \cdot \vec{X}_\beta - \vec{X}\right| \tag{48}$$

$$\vec{D}_\delta = \left|\vec{C}_3 \cdot \vec{X}_\delta - \vec{X}\right| \tag{49}$$

$$\vec{X}_1 = \vec{X}_\alpha - \vec{A}_1 \cdot \left(\vec{D}_\alpha\right) \tag{50}$$

$$\vec{X}_2 = \vec{X}_\beta - \vec{A}_2 \cdot \left(\vec{D}_\beta\right) \tag{51}$$

$$\vec{X}_3 = \vec{X}_\delta - \vec{A}_3 \cdot \left(\vec{D}_\delta\right) \tag{52}$$

$$\vec{X}(k+1) = \frac{\vec{X}_1 + \vec{X}_2 + \vec{X}_3}{3} \tag{53}$$

There is also a possibility that the newly determined location resulting from Equation (53) exceeds the bounds of variables. In the suggested MGWO, this is revised through moving randomly toward the boundary exceeding for increasing randomness, whereas in the main GWO, it is corrected by the boundary in the following way:

$$\vec{X}^j(k+1) = \begin{cases} \vec{X}^j(k) + r \cdot \left(Ub^j - \vec{X}^j(k)\right), \text{if } \left(\vec{X}^j(k+1)\right) > Ub^j \\ \vec{X}^j(k) + r \cdot \left(Lb^j - \vec{X}^j(k)\right), \text{if } \left(\vec{X}^j(k+1)\right) > Lb^j \end{cases} \tag{54}$$

In which r has been selected randomly among 0 and 1, Ub^j shows the upper bound and Lb^j indicates the lower bound of the j^{th} variable. In addition, the fitness value $f(\vec{X}^j(k+1))$ has been compared to $f(\vec{X}^j(k))$. The improved fitness value and related locations have been maintained.

Figure 2 illustrates the flowchart of this suggested algorithm for solving EM in an SH. Here are the stages that are used for solving the objective restricted issue of finding the best operating states of various loads in order to organize among the recognizable production systems in an SH.

5 | SIMULATION OUTCOMES

The following part simulates the applied EM scheme. In the optimization procedure of the scenario that has included whole systems, there would be 563 variables scheduled for a 24-h period, of which 247 would be continuous variables and 316 would be discrete variables, and it takes 0.04 s of CPU time for all iterations. For the 168-h period, there would be 3971 variables, out of which 1753 would be continuous variables and 2218 would be discrete variables, and all iterations take 0.11 s. Table 2 shows the major simulation parameters. Meteonorme 6.1″ has been used to provide the hourly solar radiation and ref. [23] for the wind speed forecast. EV has a driving electricity demand of 2 kW.

A maintenance cost of 0.01€/kWh has been selected for $C_{PV}(t)$, $C_W(t)$, $C_{EV}^{Disch}(t)$ and $C_B^{Disch}(t)$ [24]. The price of selling energy to the grid would be 0.10€/kWh, while the price of purchasing energy has been taken based on ref. [25]. It is

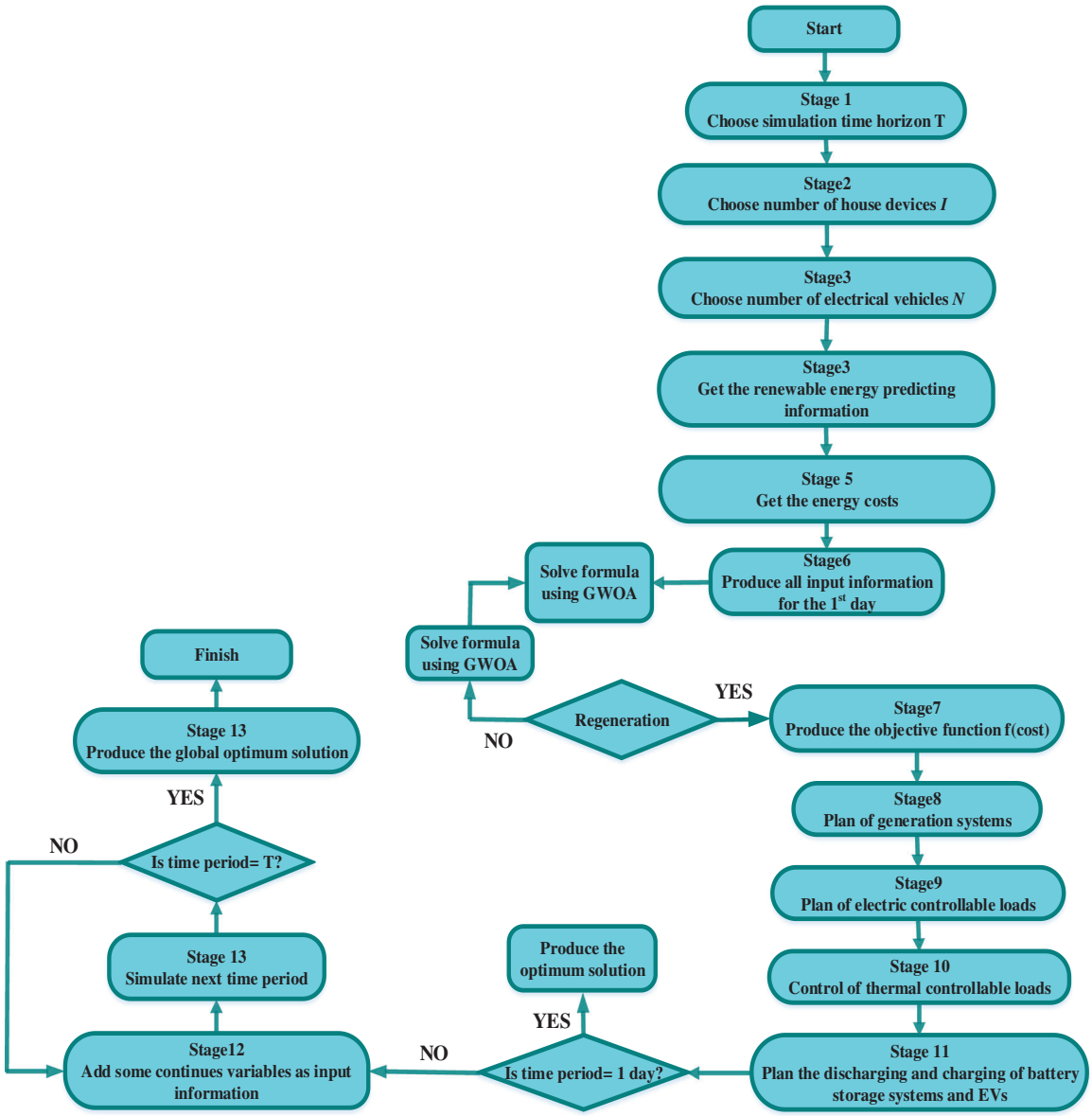

FIGURE 2 Flowchart of proposed method for consecutive day

TABLE 2 Simulation parameters

	Parameters	ρ		A_{pv}	P_{pv}^{max}	
PV	**Values**	**18.6%**		**25 m²**	**3.5 kW**	
EV	**Parameters**	$SOC_{EV}^{min}(j)$		$P_{EV}^{Cmax}(j), P_{EV}^{Dmax}(j)$	$Nom_{EV}^{int}(j)$	$Nom_{EV}(j)$
	Values	20%		3.3 kW	16 kWh	24 kWh
WT	**Parameters**	v_r	P_{rated}	P_w^{max}	v_{co}	v_{ci}
	Values	14 m/s	2.1 kW	2.4 kW	25 m/s	4 m/s
BSS	**Parameters**	e_c, e_d	SOC_B^{min}	P_B^{max}, P_B^{Dmax}	Nom_B^{int}	Nom_B
	Values	95%	20%	1 kW	6 kWh	10 kWh

TABLE 3 Suggested cases for one day

Scenario		1	2	3	4	5
V2G		×	×	√	√	√
Battery		×	×	√	√	√
Generation system	Grid	√	√	√	√	√
	RER	×	×	√	√	√
DR program	TCL	×	×	×	×	√
	ECL	×	√	×	√	√

recommended that the consumer adopts the following temperature ranges: between 3 and 8°C for the REF, between 55 and 60°C for the EWH, and between 20 and 23°C for the indoor temperature. We have made some assumptions in this work:

1. The power grid is assumed to be symmetrical load structure and thus one-phase analysis would suffice.
2. It is assumed that there is no harmonic load in the system.
3. It is assumed that the next-day load pattern consumption could be guessed properly.

A variety of cases have been presented to demonstrate lower energy costs, as well as the robustness and effectiveness of this suggested residential EM system. First, five scenarios are performed with a simulation period of 24 h, and a simulation for the final case has been performed with a longer simulation period. Please note it that as similar to other evolutionary algorithms, we have tried to provide the most fitting values for the parameters based on a sensitivity analysis. That is clear that there is no simple and straightforward method for finding the most fitting values for any of the algorithms. Instead, the most reliable and suitable method is still sensitivity analysis, which can provide promising solutions.

5.1 | Simulation for one day

Table 3 presents five scenarios, each corresponding to a simulation period of 24 h.

Scenario-1. This would be an essential case where 1 household user purchases energy solely from the network.
Scenario-2. Scenario one plus the DR program through the shift of several ECL to the intervals with lower cost.
Scenario-3. Scenario one in addition to the combination of the PV, WT, BSS and EVs.
Scenario-4. Scenario three in addition to the considering DR program through the shift of several ECL to the intervals with lower cost.
Scenario-5. Scenario four plus the DR program with TCL that could preserve several predetermined temperature at the optimum range.

Figure 3 and Table 4 reveal the outcomes of the precise solution process used to determine the lowest energy costs and operating states for a SH while organizing between the proposed generation systems. Since the DR program is integrated through ECL, there is a reduction in cost between cases one and two, from 1008.56 to 642.03€ cents. In the third scenario, the cost decreases to 34.45€ when the solar and wind system, BSS, and V2G are considered, and the user profits from the excess energy by injecting 18.57 kW into the system. Taking into account the ELC, scenario 4′s price has been reduced to −39.42€, and the amount of energy delivered to the network would be 26.66 kW. Scenario five, with the TCL applied, achieved an enormous reduction in the price, reaching −106.89€ cents. Furthermore, the network has a minimal purchasing energy of 36.28 kW and also a maximal sold energy of 29.52 kW. For each case, the computation time would be small, but it rises in the last case in which the whole of the systems are controlled and scheduled.

TABLE 4 Simulation outcomes for one day

Scenario	1	2	3	4	5
Price (€ cents)	1009	642	35	−39	−107
Computation time (s)	0.3	0.5	0.3	0.5	16
Sold power (kW)	–	–	18.6	26.7	29.5
Bought power (kw)	64.7	64.7	36.8	45.3	36.3

5.2 | Simulating consecutive days

A similar EM model as in case five has been executed for a simulation period of 24 h, 48 h, 72 h, 96 h, 120 h, 144 h, and 168 h for each system. Table 5 compares the MILP or the precise solution and the GWOA discussed in Section 4 in order to minimize energy costs and computation time. It can be observed that in the simulation period of 24, the optimum solution with the MILP and a sufficient computing time is 16.23 and in the simulation period of 48, the optimum solution with the MILP and a sufficient computing time is 49.39 s. For the rest, the simulation would be terminated at 600 s to find near-optimum solutions. As a result, by applying a GWOA, a solution would be found for the challenging formulation, and a majority of the outcomes over the various periods would be similar to those achieved by MILP. There is a dramatic reduction in computation time in every scenario; in particular, there is a decrease of 94% from 600 s to 35.18 s in the 72 h simulation time. Using the 48-h period, the minimal gap has been calculated as −4.60 %, with the optimum outcome with the MILP algorithm being −99.93€ cents and with the GWOA being −95.33€ cents.

In the case of surplus power that is sold to the grid, the value of the objective function would not be positive. Figure 4 illustrates the EM for the total sources of the 48-h period in which the whole generation and usage systems have been planned to meet every constraint. Therefore, the GWOA could obtain a good solution with a minimal run time and within a suitable tolerance if the precise approach cannot.

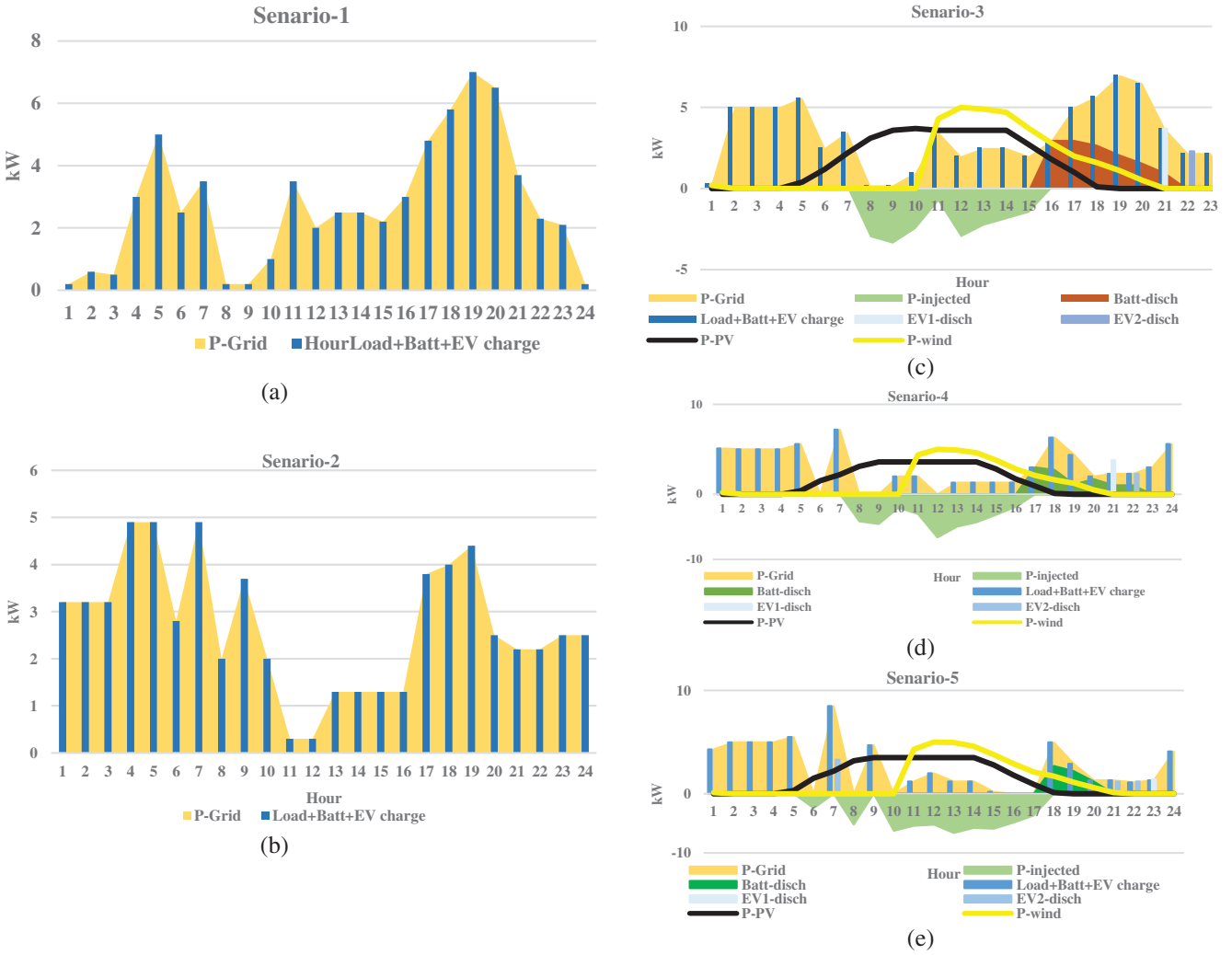

FIGURE 3 EM for single day: (a) Senario-1; (b) Senario-2; (c) Senario-3; (d) Senario-4; (e) Senario-5

TABLE 5 Simulation outcomes of consecutive day

Scenario		5						
Period (h)		24	48	72	96	120	144	168
F (cost)	GWOA (€ cents)	–	−95.4	−83.1	−60.9	−38.8	−19.5	4.7
	Gap (%)	–	−4.7	−6.9	−4.6	−6.9	−8.6	23.1
	MILP (€ cents)	−107.2	−99.7	−89.9	−66.4	−44.1	−22.2	4.1
Computation time	GWOA (s)	–	25.5	347	68.7	77.9	88.1	175.1
	MILP (s)	16.23	49.39	600	600	600	600	600

6 | ALGORITHM EFFICIENCY ASSESSMENT

This paper tests and evaluates the efficiency and effectiveness of the GWOA by using various curves of the purchasing price, illustrated in Figure 5. Five curves are chosen at random, every one of which was simulated with whole periods as shown in Table 6: 48, 72, 96, 120, 144, and 168 h. During a 48-h simulation, the average of outcomes achieved using MILP would be 190.97€ cents, whereas the solution of the GWOA would be 194.70€ cents with a gap of 1.95%. There is a 90% reduction in computation time from 164.26 to 16.15 s. A 72-h simulation period has an average of 395.53€ cents achieved with MILP compared to 402.08€ cents achieved by the GWOA with a gap

TABLE 6 Simulation outcomes for various price curve

Scenario		**5**					
Period		**48**	**48**	**48**	**48**	**48**	**Average**
***N*° of price curve**		**1**	**2**	**3**	**4**	**5**	
F (cost)	GWOA (€ cents)	301.5	344.7	188.7	161.8	−22.8	194.8
	Gap (%)	3.1	2.6	0.1	0.5	−0.7	1.1
	MILP (€ cents)	294.4	341.2	189.7	159.7	−23.9	192.2
Computation time	GWOA (s)	16.7	6.3	17.1	16.9	24.2	16.2
	MILP (s)	600	11.8	45.2	33.1	137.2	165.5
Scenario		**5**					
Period		**72**	**72**	**72**	**72**	**72**	**Average**
***N*° of price curve**		**1**	**2**	**3**	**4**	**5**	
F (cost)	GWOA (€ cents)	579.4	639.8	409.7	341.2	32.5	401.9
	Gap (%)	2.9	2.6	0.3	0.1	-3.1	0.6
	MILP (€ cents)	565.9	631.2	409.8	341.2	33.6	396.3
Computation time	GWOA (s)	16.1	11.9	10.8	19.2	35.3	18.7
	MILP (s)	17.4	22.5	12.9	46.1	600	139.8
Scenario		**5**					
Period		**96**	**96**	**96**	**96**	**96**	**Average**
***N*° of price curve**		**1**	**2**	**3**	**4**	**5**	
F (cost)	GWOA (€ cents)	879.1	968.1	639.6	499.5	93.7	616
	Gap (%)	3.6	3.5	−0.8	−5.2	−6.4	1.1
	MILP (€ cents)	856.1	938.2	648.1	532.8	109.8	617
Computation time	GWOA (s)	18.8	14.2	18.9	54.2	15.9	24.4
	MILP (s)	600	600	600	600	600	600
Scenario		**5**					
Period		**120**	**120**	**120**	**120**	**120**	**Average**
***N*° of price curve**		**1**	**2**	**3**	**4**	**5**	
F (cost)	GWOA (€ cents)	1198.4	1308.2	879.8	684.3	158.9	845.9
	Gap (%)	6.3	6.2	1.4	−4.2	−4.3	1.1
	MILP (€ cents)	1128.2	1233.5	869.4	709.7	165.9	821.3
Computation time	GWOA (s)	24.1	20.1	25.9	35.9	62.9	33.8
	MILP (s)	600	600	151.2	600	600	510.2
Scenario		**5**					
Period		**144**	**144**	**144**	**144**	**144**	**Average**
***N*° of price curve**		**1**	**2**	**3**	**4**	**5**	
F(cost)	GWOA (€ cents)	1499.7	1641.6	1122.3	861.6	225.8	1070.2
	Gap (%)	7.2	7.2	2.2	−3.6	−3.9	1.8
	MILP (€ cents)	1398.9	1531.2	1101.2	891.5	229.8	1030.5
Computation time	GWOA (s)	29.1	19.8	28.9	63.4	155.7	59.4
	MILP (s)	228	113.4	72.7	600	600	322.8
Scenario		**5**					
Period		**168**	**168**	**168**	**168**	**168**	**Average**
***N*° of price curve**		**1**	**2**	**3**	**4**	**5**	
F (cost)	GWOA (€ cents)	1831.8	1985.2	1358.7	1033.5	294.6	1300.8
	Gap (%)	7.9	7.9	2.3	−3.7	−4.6	2
	MILP (€ cents)	1702.4	1838.4	1329.3	1078.5	311.7	1252.1
Computation time	GWOA (s)	25.7	17.8	25.3	77.7	88.2	46.9
	MILP (s)	600	600	600	600	600	600

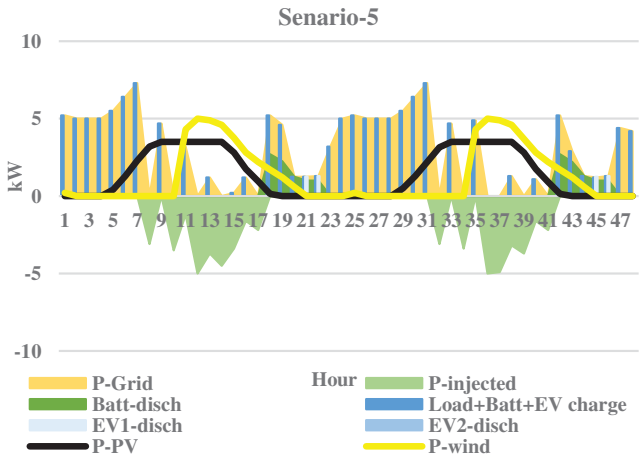

FIGURE 4 EM of 48-h period

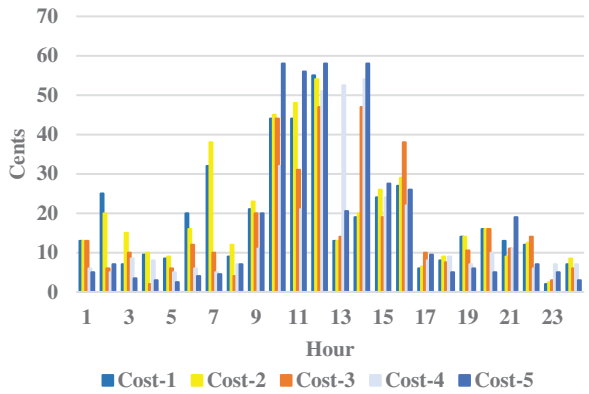

FIGURE 5 Various price curves

of 1.66%. This reduces computation time by 87% from 139.46 to 18.40 s. A 96-h simulation time horizon yields the following average result: 616.34€ cents with MILP while 621.31€ cents with the GWOA with a gap of 0.81%.

There is a 96% decrease in computation time from 600 s to 24.37 s. A 120-h simulation period obtains an average of 823.56€ cents using MILP, and 848.03€ cents using GWOA, with a gap of 2.97%. There is a 93% decrease in computing time from 509.79 to 33.67 s. A 144-h simulation period gives an average of 1030.08€ cents for MILP and 1069.20€ cents for GWOA; the gap is 3.80%. There is 82% decrease in computation time from 321.06 s to 59.16 s. Lastly, a 168-h simulation period gives an average of 1250.76€ cents for MILP and 1301.45€ cents for GWOA; the gap is 4.05%. There is a 92% reduction in computation time from 600 to 47.09 s. The outcomes demonstrate that this suggested GWOA works efficiently and would be adaptive to the factor variation since the global optimum solution would be close to the optimum solution in whole cases in simulating consecutive days. In addition, the computation time is significantly reduced, which is important in real-time applications.

7 | CONCLUSION

The study proposes a new EM system that takes into account production as well as usage systems. Within the scheme, renewable energy sources can be scheduled with the grid at generation, and after that, various thermal and electric devices, batteries, and EVs can be controlled and managed. An optimization algorithm has also been applied to address the issue of long-term simulations, which will decrease consumers' energy bills in SHs for consecutive days. The efficiency of this suggested method would be demonstrated by comparing it with a GWOA. According to outcomes, the optimal solution would be found in scenario five, in which the TCL adjusts the REF, EWH, and room temperature for minimizing the power usage and maintaining the lowest satisfaction level. Moreover, the outcomes demonstrate that this suggested optimization algorithm is capable of obtaining a close-to-optimum solution with a strong reduction in computation time. Numerous SHs will be considered in future research for adapting microgrid EM systems. The results show that more than 50% improvement could be made for the energy management part. The main limitation of the proposed model is its ability for handling the centralized structure problems. In other words, the proposed problem formulation is not structured for the decentralized or distributed models. Moreover, the model performance relies on the searchability of the evolutionary algorithms. This can be assessed in the future works.

AUTHOR CONTRIBUTIONS

A.M.: Conceptualization; Data curation; Formal analysis. M.M.: Investigation; Project administration; Resources; Software; Writing-original draft. M.K.: Software; Supervision; Validation. A.B.: Validation; Visualization; Writing-original draft; Writing-review & editing.

CONFLICT OF INTEREST

The authors declare no conflict of interest.

FUNDING INFORMATION

The authors received no specific funding for this work.

DATA AVAILABILITY STATEMENT

Data available on request from the authors.

ORCID

Mohammadamin Mobtahej https://orcid.org/0000-0001-8963-6723

Mazaher Karimi https://orcid.org/0000-0003-2145-4936

REFERENCES

1. Dabb, M., Kavousi-Fard, A., Yang Dong, Z.: A novel distributed cloud-fog based framework for energy management of networked microgrids. IEEE Trans. Power Syst. 35(4), 2847–2862 (2020)
2. Mohammadi, M., Kavousi-Fard, A., Dehghani, M., Karimi, M., Loia, V., Alhelou, H.H., Siano, P.: Reinforcing data integrity in renewable hybrid AC-DC microgrids from social-economic perspectives. ACM Trans. Sens. Netw. 99, 1–14 (2022)

3. Jokar, H., Bahmani-Firouzi, B., Simab, M.: Bilevel model for security-constrained and reliability transmission and distribution substation energy management considering large-scale energy storage and demand side management. Energy Rep. 8, 2617–2629 (2022)
4. Mahto, N.K., Jaiswal, S., Das, D.C.: Demand-side management approach using heuristic optimization with solar generation and storage devices for future smart grid. In: Renewable Energy Towards Smart Grid. pp. 407–420. Springer, Singapore (2022)
5. Kavousi-Fard, A., Niknam, T., Akbari-Zadeh, M.R., Dehghan, B.: Stochastic framework for reliability enhancement using optimal feeder reconfiguration. J. Syst. Eng. Electron. 25(5), 901–910 (2014)
6. Mostafa, N., Ramadan, H.S.M., Elfarouk, O.: Renewable energy management in smart grids by using big data analytics and machine learning. Mach. Learn. Appl. 9, 100363 (2022)
7. Ruan, G., Zhong, H., Wang, J., Xia, Q., Kang, C.: Neural-network-based Lagrange multiplier selection for distributed demand response in smart grid. Appl. Energy 264, 114636 (2020)
8. Parvin, K., Hannan, M.A., Dong, Z.Y.: The future energy internet for utility energy service and demand-side management in smart grid: Current practices, challenges and future directions. Sustainable Energy Technol. Assess. 53, 102648 (2022)
9. Mbungu, N.T., Bansal, R.C., Naidoo, R., Miranda, V., Bipath, M.: An optimal energy management system for a commercial building with renewable energy generation under real-time electricity prices. Sustainable Cities Soc. 41, 392–404 (2018)
10. Abdelrahman, O., AliMohamed, R., ElmarghanyAhmed, M.H.: Closed-loop home energy management system with renewable energy sources in a smart grid: A comprehensive review. J. Energy Storage 50, 104609 (2022)
11. Basu, M.: Fast convergence evolutionary programming for economic dispatch problems. IET Gener., Transm. Distrib. 11(16), 4009–4017 (2017)
12. Basu, M.: Modified particle swarm optimization for nonconvex economic dispatch problems. Int. J. Electr. Power Energy Syst. 69, 304–312 (2015)
13. Larik, R.M., Mustafa, M.W., Aman, M.N., Jumani, T.A., Sajid, S., Panjwani, M.K.: An improved algorithm for optimal load shedding in power systems. Energies 11(7), 1808 (2018)
14. Tang, R., Wang, S., Li, H.: Game theory based interactive demand side management responding to dynamic pricing in price-based demand response of smart grids. Appl. Energy 250, 118–130 (2019)
15. Zhang, Y., Rahbari-Asr, N., Chow, M.Y.: A robust distributed system incremental cost estimation algorithm for smart grid economic dispatch with communications information losses. J. Network Comput. Appl. 59, 315–324 (2016)
16. Kouveliotis-Lysikatos, I., Hatziargyriou, N.: Fully distributed economic dispatch of distributed generators in active distribution networks considering losses. IET Gener., Transm. Distrib. 11(3), 627–636 (2017)
17. Nudell, T.R., Brignone, M., Robba, M., Bonfiglio, A., Ferro, G., Delfino, F., Annaswamy, A.M.: Distributed control for polygeneration microgrids: A dynamic market mechanism approach. Control Eng. Pract. 121, 105052 (2022)
18. Mehrabani, A., Mardani, H., Ghazizadeh, M.S.: Optimal energy management in smart home considering renewable energies, electric vehicle, and demand-side management. In: 2022 9th Iranian Conference on Renewable Energy & Distributed Generation (ICREDG). Shiraz, Iran. pp. 1–5 (2022)
19. Sterling, G., Tyler, B.: Renewable energy management using action dependent heuristic dynamic programming. In: 2018 IEEE International Smart Cities Conference (ISC2). Paphos, Cyprus, pp. 1–5 (2018)
20. Shen, L., Li, J., Wu, Y., Tang, Z., Wang, Y.: Optimization of artificial bee colony algorithm based load balancing in smart grid cloud. In: 2019 IEEE Innovative Smart Grid Technologies-Asia (ISGT Asia). Chengdu, China, pp. 1131–1134 (2019)
21. Mirjalili, S., Mirjalili, S.M., Lewis, A.: Grey wolf optimizer. Adv. Eng. Software 69, 46–61 (2014)
22. Heidari, A.A., Pahlavani, P.: An efficient modified grey wolf optimizer with Lévy flight for optimization tasks. Appl. Soft Comput. 60, 115–134 (2017)
23. Cho, S.M., Kim, J.S., Kim, J.C.: Optimal operation parameter estimation of energy storage for frequency regulation. Energies 12(9), 1782 (2019)
24. Ghiasi, M., Niknam, T., Dehghani, M., Siano, P., Haes Alhelou, H., Al-Hinai, A.: Optimal multi-operation energy management in smart microgrids in the presence of ress based on multi-objective improved de algorithm: Cost-emission based optimization. Appl. Sci. 11(8), 3661 (2021)
25. Osório, G.J., Shafie-khah, M., Coimbra, P.D., Lotfi, M., Catalão, J.P.: Distribution system operation with electric vehicle charging schedules and renewable energy resources. Energies 11(11), 3117 (2018)

How to cite this article: Maroufi, A., Mobtahej, M., Karimi, M., Baziar, A.: A novel energy management model among interdependent sections in the smart grids. IET Gener. Transm. Distrib. 1–13 (2022). https://doi.org/10.1049/gtd2.12702